Title	Ammonia storage materials for nitrogen recycling hydrogen and energy carriers
Author(s)	Kojima, Yoshitsugu; Yamaguchi, Masakuni
Citation	International Journal of Hydrogen Energy , 45 (16) : 10233 - 10246
Issue Date	2020-03-20
DOI	10.1016/j.ijhydene.2020.01.145
Self DOI	
URL	https://ir.lib.hiroshima-u.ac.jp/00050470
Right	© 2020. This manuscript version is made available under the CC-BY-NC-ND 4.0 license http://creativecommons.org/licenses/by-nc-nd/4.0/ This is not the published version. Please cite only the published version. この論文は出版社版ではありません。引用の際には出版社版をご確認、ご利用ください。
Relation	

Ammonia Storage Materials for Nitrogen Recycling Hydrogen and Energy Carriers

Yoshitsugu Kojima [a, b], *, Masakuni Yamaguchi [b]

[a] *Natural Science Center for Basic Research and Development, Hiroshima University, 1-3-1, Kagamiyama, Higashi-Hiroshima, Hiroshima 739-8530, Japan*

[b] *Graduate School of Advanced Sciences of Matter, Hiroshima University, 1-3-1, Kagamiyama, Higashi-Hiroshima, Hiroshima 739-8530, Japan*

Abstract

Ammonia (NH_3) has large gravimetric and volumetric H_2 densities and has advantages as hydrogen and energy carriers. Unfortunately, NH_3 is a deleterious substance. NH_3 storage technology is essentially necessary to suppress leaked NH_3 in the atmosphere. Many kinds of NH_3 storage materials, which are metal halides, borohydrides, ammonia borane, proton-based materials, porous materials and water have been studied. In those materials, water easily collects leaked NH_3 because of the large diffusion coefficient of NH_3. H^+ in proton-based materials can react with lone electron pair of NH_3 to form NH_4^+ and has low NH_3 vapor pressure in the atmosphere. Insoluble proton-based materials also can remove nitrogen (NH_3-N) from NH_3 water. Therefore the NH_3 removal system combined water and insoluble proton-based materials will be candidate for the leaked NH_3 concentration lowering in the atmosphere by suppression of water pollution.

Keywords: ammonia storage materials; proton-based materials; water; ammonia removal system.

*** Corresponding author. Tel.: +81 82 424 3904; fax: +81 82 424 5744.**

E-mail address: **kojimay@hiroshima-u.ac.jp (Y. Kojima).**

---

1. Introduction

Hydrogen is produced from renewable energy by electrolysis of water and thermochemical water splitting. Unfortunately, hydrogen is a gas at room temperature, hydrogen storage materials (hydrogen carriers) are key to realize uniform renewable energy for global leveling. Ammonia (NH_3) is easily liquefied by compression at 1 MPa and 298 K, and has a high gravimetric H_2 density of 17.8 wt% and highest volumetric hydrogen density which is above 1.5 times of liquid H_2 [1]. NH_3 is also burnable substance. The theoretical hydrogen conversion efficiency of NH_3 is 89.3% [1], which is close value to that of conventional $LaNi_5$ alloy (88.8%).

According to IEA report, the cost of importing NH_3 from electrolytic hydrogen produced in Australia into Japan 2030 as a hydrogen carrier is low compared with liquid hydrogen and organic hydrides (methyl cyclohexane, toluene) [2]. If NH_3 could be used by the end user without the need for reconversion, the cost would be even lower.

Thus, NH_3 has advantages as nitrogen recycling hydrogen and energy carriers for renewable energy [1, 2]. Unfortunately, NH_3 is a deleterious substance. NH_3 storage materials will have a key role to suppress the leaked NH_3 in the atmosphere. Figure 1 shows structure models of NH_3 storage materials. These materials such as metal halides, porous materials and proton-based materials have been studied for energy storage [3], refrigeration [3], heat-pumping [3], NO_x reduction [4] and hydrogen purification [5].

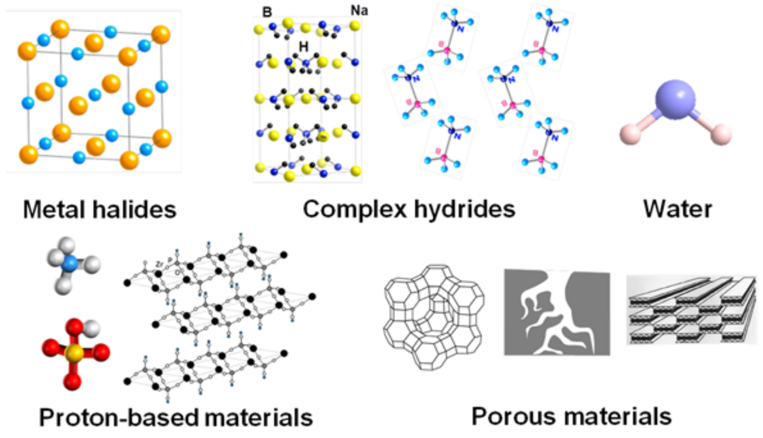

Figure 1. Structure models of NH_3 storage materials.

In this study, safety of NH_3 is considered. Then, we focused on NH_3 storage materials as a NH_3 remover. We will overview experimental and theoretical results on NH_3 storage properties of metal halides, complex hydrides (borohydrides, ammonia borane), proton-based materials, porous materials and water to suppress leaked NH_3 in the atmosphere. We will also propose new concept of NH_3 removal system to decrease leaked NH_3

concentration.

2. Safety of NH_3

Safety of NH_3 will be classified into flammability and health hazard. The regulations for flammability and health hazard are defined in each region. Major standard regulations in each region are Japanese GHS (The Globally Harmonized System of Classification and Labelling of Chemicals), NFPA (National Fire Protection Association) 704 in USA, CLP (Classification, Labelling and Packaging of substances and mixtures) in Europe. We evaluated correlation between flammability and the properties of the hydrogen carriers. NFPA 704 defines "Fire Diamond" used by emergency personnel to quickly and easily identify the risks posed by hazardous materials.

NFPA flammability of NH_3 is low value of 1 because of high flash point (405 K) [6]. The flammability increases with decreasing of the flash point. Hydrogen and organic hydrides have high values of 3-4 because of lower flash points (flash point of H_2: 20 K, flash point of methylcyclohexane: 267 K, flash point of toluene: 277 K) [6, 7]. The CLP and Japanese GHS flammabilities also have similar trend except the value of NH_3 in Japanese GHS. This is due to the fact that the classification of flammability obtained by Japanese GHS is defined by explosive limit in air.

Human nose can detect NH_3 at 5-20 ppm [8, 9]. American Conference of Governmental Industrial Hygienists (ACGIH) threshold limit value (TLV) for an 8 hour time weighted average (TWA) exposure is 25 ppm (18 mg/m^3)[8]. NFPA health hazard increases with the solubility in water and the value of NH_3 has high value of 3. The solubility of hydrogen in water is small. Thus, the health hazard of hydrogen gas obtained by NFPA 704 has low value of 0. Unfortunately, H_2 gas cannot be used for large amount of hydrogen transportation.

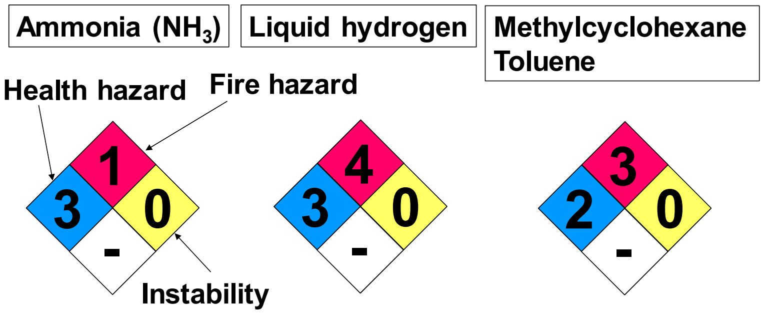

Figure 2. Fire diamonds of NH_3, liquid hydrogen and organic hydrides (methylcyclohexane, toluene) as hydrogen carriers

Fire diamonds of hydrogen carriers such as NH_3, liquid hydrogen and organic hydrides are shown in Figure 2. NFPA health hazard of liquid H_2 has high value 3 because of suffocation death due to lack of oxygen and frostbite [10], which is the same as NH_3. The NFPA health hazard of organic hydride (methyl cyclohexane and toluene) is 2. The CLP health hazards of NH_3 and organic hydrides are high and similar to those in Japanese GHS.

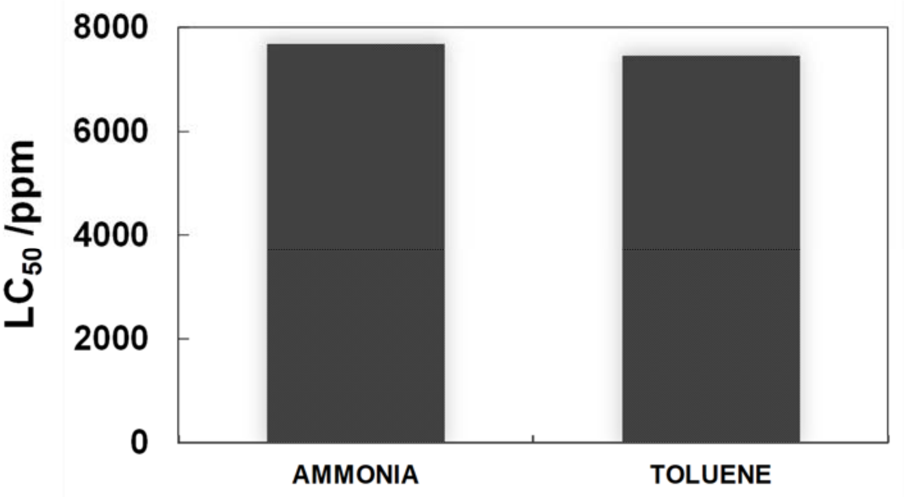

Figure 3. LC_{50} (50% lethal concentration, 4 h rat inhalation) of ammonia and toluene.

Figure 3 shows LC_{50} (50% lethal concentration, 4 h rat inhalation) of NH_3 and toluene which is a byproduct of organic hydride [6]. The LC_{50} of NH_3 and toluene are 7679 ppm and 7460 ppm, respectively [6]. Thus, it is assumed that the health hazards of these 3 kinds of hydrogen carriers have same level.

3. NH_3 storage materials as a remover

NH_3 accident occurred in Japan 2014 is only in the plant facilities. The ratio of NH_3 accidents divided by the high pressure gas accidents is about 10%. All accidents with NH_3 are caused by leaks from valve, pipe and flange in the plant facilities [11]. The maximum NH_3 vapor concentration is 2 ppm (vapor pressure: 0.2 Pa at atmospheric pressure) based on an offensive odor control law at industrial area in Japan [12]. This indicates that the required properties of NH_3 storage materials as a remover are low equilibrium NH_3 pressure (plateau pressure) of 0.2 Pa and large NH_3 storage capacity.

NH_3 storage materials store NH_3 in the form of ammine [13], ammonium ion (NH_4^+) [14] and NH_3 molecule [15]. Metal halides and complex hydrides form metal ammine complex salts. Proton-based materials store NH_3 in the form of ammonium ion by the coordinate bond between H^+ and lone pair of electron in NH_3. Porous materials adsorb NH_3 and water absorbs NH_3 in the form of molecules.

3.1 Metal Halides

Metal halides composed of metals and halogen are considered as the attractive NH_3 storage materials because they form metal ammine complex salts. NH_3 is coordinated to the metal and is called as a ligand [13]. NH_3 absorption of metal halides are expressed by the following equation [13, 16-34]

$$MX_m + n\mathrm{NH_3} \rightarrow M(\mathrm{NH_3})_n X_m \quad (1)$$

M: Li, Na (m=1), Mg, Ca, Mn, Co, Ni, Cu, Zn, Sr, Ba, Ag (m=2), Co (m=3), Pt (m=4) etc., X: Cl, Br, I, n: 1, 2, 4, 6, 8, where n is coordination number.

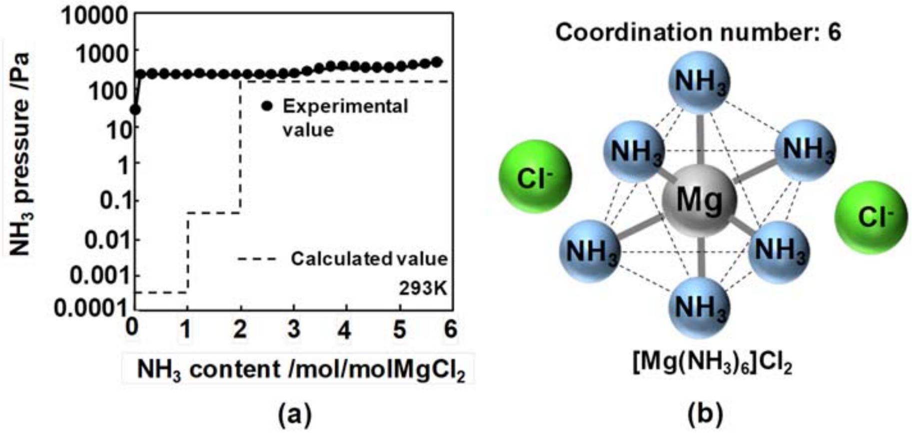

Figure 4. Pressure-composition (P-C) isotherms for $MgCl_2$-NH_3 system and the structure model of the hexa-ammine complex salt $Mg(NH_3)_6Cl_2$ [13, 18].

NH_3 absorption properties of $MgCl_2$ have been studied due to its high NH_3 storage capacity of 52 wt%. Figure 4 (a) shows experimental and calculated pressure-composition (P-C) isotherms for $MgCl_2$-NH_3 system and the structure model of the hexa-ammine complex salt [13, 18]. The hexa-ammine complex salt is directly formed at 293 K by reaction $MgCl_2$ and NH_3 without formation of mono- and di-ammine complex salts [$Mg(NH_3)Cl_2$, $Mg(NH_3)_2Cl_2$]. This suggests the presence of large activation barrier to form ammine complex salts with low coordination number [18].

Table 1 shows theoretical gravimetric NH_3 density, plateau pressure in metal halide-NH_3 systems (metal halide ammine complex salts). The gravimetric NH_3 densities are 7-62 wt%. The calculated plateau pressure of metal ammine complex salts such as $Mg(NH_3)Cl_2$, $Mg(NH_3)_2Cl_2$, $Mn(NH_3)Cl_2$, $Mn(NH_3)Br_2$ with the coordination number 1-2 is below 0.2 Pa, which satisfies the regulation value of the offensive odor control law at industrial area in Japan.

Table 1. Theoretical gravimetric NH_3 density, plateau pressure, standard enthalpy change and standard entropy change in metal halide-NH_3 systems (metal halide ammine complex salts).

Metal halides	Metal ammine complex	Theoretical gravimetric NH_3 density /wt%	Plateau pressure /Pa(293-298K)	Standard enthalpy change ΔH^0 /kJ/molNH_3	Standard entropy change ΔS^0 /J/KmolNH_3
LiCl	$Li(NH_3)_4Cl$	61.6	178000 (293K) [17,19]	-34 [17]	-119 [17]
NaCl	-	-	>800000 (293K) [17,19]	-	-
LiF	-	*	>800000 (293K) [17,19]	-	-
LiBr	-	-	<1000 (293K) [17,19]	-	-
NaI	$Na(NH_3)_5I$	36.2	55000 (293K) [17,19]	-	-
$MgCl_2$	$Mg(NH_3)Cl_2$ $Mg(NH_3)_2Cl_2$ $Mg(NH_3)_6Cl_2$ $Mg(NH_3)_6Cl_2$ $Mg(NH_3)Cl_2$	15.2 26.3 51.8 51.8 15.2	0.000645^* (298K) [16] 0.0804^{**} (298K) [16] 197^{**} (298K) [16] 500 (293K) [18] 0.0706^* (293K) [18]	-87.0 [16,22] -74.9 [16,22] -55.6 [16,22] -58 [18] -64 [18]	-135 [16,22] -135 [16,22] -135 [16,22] -150 [18] -97 [18]
$CaCl_2$	$Ca(NH_3)Cl_2$ $Ca(NH_3)_2Cl_2$ $Ca(NH_3)_4Cl_2$ $Ca(NH_3)_8Cl_2$ $Ca(NH_3)_8Cl_2$	13.3 23.5 38.0 55.1 55.1	1.36^* (298K) [16] 21.2^* (298K) [16] 40300^* (298K) [16] 69900^* (298K) [16] 22000 (293K) [17,19]	-69.0 [16] -63.2 [16] -42.3 [16] -41.0 [16] -	-138 [16] -142 [16] -134 [16] -135 [16] -
$CaBr_2$	$Ca(NH_3)_8Br_2$	40.5	7000 (293K) [17,19]	-	-
$MnCl_2$	$Mn(NH_3)Cl_2$ $Mn(NH_3)_2Cl_2$ $Mn(NH_3)_6Cl_2$	11.9 21.3 44.8	0.0201^* (298K) [26] 3.82^* (298K) [26] 2700 (293K) [17,19], 31000^* (298K) [26]	-84.1 [26] -71.1 [26] -47.3 [26]	-154 [26] -154 [26] -149 [26]
$MnBr_2$	$Mn(NH_3)Br_2$ $Mn(NH_3)_2Br_2$ $Mn(NH_3)_6Br_2$	7.35 13.7 32.2	0.0236^* (298K) [26] 0.277^* (298K) [26] 3370^* (298K) [26]	-83.7 [26] -77.0 [26] -53.1 [26]	-150 [26] -152 [26] -154 [26]
$NiCl_2$	$Ni(NH_3)_6Cl_2$	44.1	60 (293K) [17,19]	-	-
NiI_2	$Ni(NH_3)_6I_2$	24.6	40 (293K) [17,19]	-	-
$SrCl_2$	$Sr(NH_3)_2Cl_2$ $Sr(NH_3)_8Cl_2$	17.7 46.2	5800^* (298K) [27] 50800^* (298K) [27], 49300^* (298K) [16]	-58.9 [27] -43.4 [27], -41.4 [16]	-174 [27] -140 [27], -133 [16]
$BaCl_2$	$Ba(NH_3)_8Cl_2$	39.6	127000 (293K) [17,19], 187000^* (298K) [6]	-37.7 [16]	-132 [16]

* Calculated value at 298K from ΔH^0 and ΔS^0

The plot of the logarithm of the plateau pressure against the reciprocal of the absolute temperature is commonly called a van't Hoff plot. The standard enthalpy change (ΔH^0) and the standard entropy change (ΔS^0) of NH_3 absorption reaction were estimated by the following van't Hoff equation (2) [17].

$$\ln\frac{P}{\mathrm{P}_0} = \frac{\Delta H^0}{RT} - \frac{\Delta S^0}{R} \tag{2}$$

where p is the plateau pressure of metal ammine complex salt (Pa), $\mathrm{P_0}$ is the standard pressure (1×10^5 Pa), R is the gas constant (8.314 J/Kmol), T is the temperature (K).

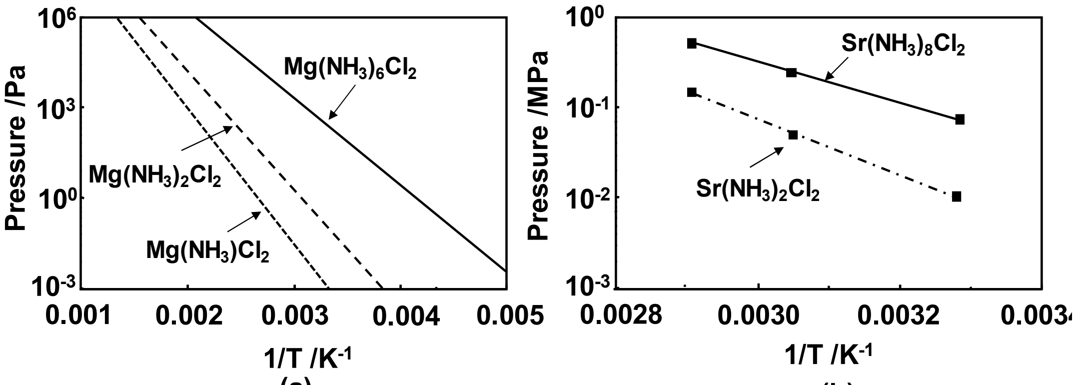

(a) (b)

Figure 5. van't Hoff plots of mono-, di-, hexa-ammine phases of $MgCl_2$, and di-, octa-ammine phases of $SrCl_2$ [22, 27].

Van't Hoff plots of $MgCl_2$-NH_3 system are shown in Figure 5 (a) [22]. The standard enthalpy change (standard heat of formation) ΔH^0 and the standard entropy change ΔS^0 of the $MgCl_2$ ammine complex salts calculated by Figure 5(a) were -87.0 (NH_3:1-0), -74.9 (NH_3:2-1), -55.6 kJ/molNH_3 (NH_3:6-2), -135 (NH_3:1-0), -134 (NH_3:2-1), -135 J/KmolNH_3 (NH_3:6-2), respectively. The absolute values of ΔS^0 are smaller than the reported values [230.9 (NH_3:1-0), 230.3 (NH_3:2-1), 230.6 J/KmolNH_3 (NH_3:6-2)] and the difference is 96 J/KmolNH_3 [16, 22].

The van't Hoff plots of $SrCl_2$-NH_3 system are shown in Figure 5 (b) [27]. The standard enthalpy change ΔH^0 and the standard entropy change ΔS^0 of the $SrCl_2$ ammine complex salts calculated by Figure 5(b) were -58.9 (NH_3:2-1), -43.4 kJ/molNH_3 (NH_3:8-2), -174 (NH_3:2-1), -140 (NH_3:8-2) J/KmolNH_3, respectively. The absolute values of ΔS^0 are also smaller than the reported value (270.1, 235.6 J/KmolNH_3) and the difference is 96 J/KmolNH_3 [27]. Equation (2) shows that

$$\ln\frac{P}{10^5} = \frac{\Delta H^0}{\mathrm{R}T} - \frac{\Delta S^0}{\mathrm{R}} \tag{3}$$

$$\ln P = \frac{\Delta H^0}{\mathrm{R}T} - \frac{\Delta S^0 + 95.7}{\mathrm{R}} \tag{4}$$

When the unit of pressure (P) is analyzed in Pa, it is predicted from equation (4) that ΔS^0 shifts by 95.7 J/KmolNH$_3$. In this paper, we revised the entropy of magnesium calcium and strontium ammine chlorides according to equation (4).

Table 1 shows standard enthalpy change and revised standard entropy change in metal halide-NH$_3$ systems. The absolute value of the standard enthalpy change of those metal ammine complex salts decreases with the coordination number. The van't Hoff plot such as Mg(NH$_3$)Cl$_2$, Mg(NH$_3$)$_2$Cl$_2$, Mn(NH$_3$)Cl$_2$ and Mn(NH$_3$)Br$_2$ with the coordination number 1-2 indicates that the standard enthalpy changes ΔH^0 are -64 to -87 kJ/molNH$_3$. (Table 1). The revised standard entropy changes of these metal ammine complex salts are in the range of -97 to -154 J/KmolNH$_3$.

The crystal structure and dynamics of Mg(ND$_3$)$_6$Cl$_2$ have been investigated by powder neutron diffraction and molecular dynamics [35]. The powder diffraction data can be well described by 4 partly occupied deuterium sites in a square arrangement around the N atoms, which is seemingly inconsistent with the 3-fold symmetry of the ND$_3$ molecule. Molecular dynamics show highly correlated rotational and translational motion of the ND$_3$ molecules [35]. It is reported from density functional theory (DFT) that the rotation of NH$_3$ in the hexa-ammine complex salt requires an activation energy of 0.09 eV in the low temperature phase of Mg(NH$_3$)$_6$Cl$_2$ and 0.002–0.12 eV in the high temperature phases, effectively [36]. NH$_3$ absorption and desorption behaviors were studied for CaCl$_2$-CaBr$_2$ halide mixtures with various molar ratios. The samples absorbed two molecules of NH$_3$ coordination [37]. The mixing effect of alkaline earth metal halides on NH$_3$ absorption−desorption behavior was studied. CaCl$_2$−CaBr$_2$ showed a pronounced NH$_3$ storage capacity (21.8 wt%) under the pressure-swing conditions of 60 and 10 kPa at 298 K, which was 12.6 times as high as that of the Na form of the Y-zeolite [38]. It is well known that CuSO$_4$ absorbs NH$_3$ to form ammine complex salt in NH$_3$ water. CuSO$_4$ also react with anhydrous NH$_3$ gas to form Cu(NH$_3$)$_n$SO$_4$ (n:1-5)(NH$_3$: 10-35 wt%)[39]. CuSO$_4$ absorbs NH$_3$ vapor concentration of 0.4 ppm or less [40]. Recently, it has been reported that ammonium halides reversibly absorb and desorb NH$_3$. The plateau pressure was 0.35 MPa [41].

3.1.1 Standard enthalpy difference and electronegativity of metal in metal halide-ammonia system

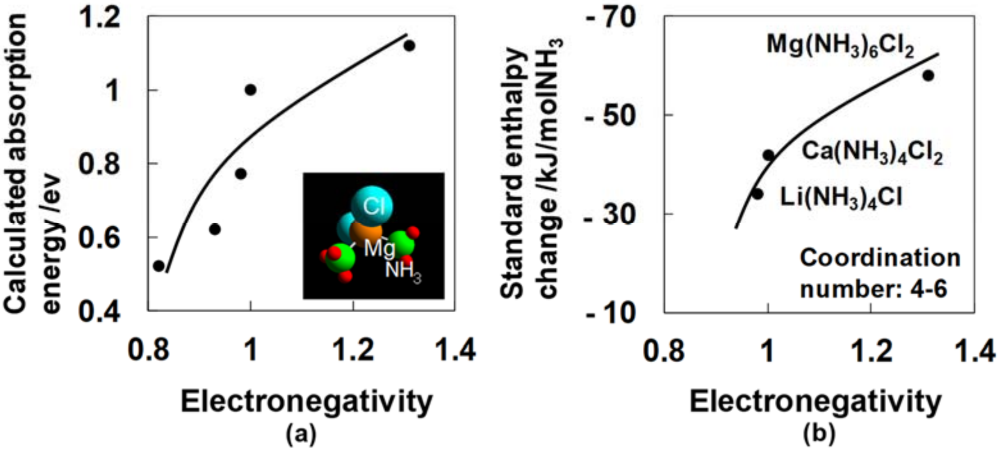

Figure 6(a). Relation between calculated absorption energy and electronegativity of metal in 2LiCl-2NH$_3$, 2NaCl-2NH$_3$, 2KCl-2NH$_3$, MgCl$_2$-2NH$_3$, CaCl$_2$-2NH$_3$, Figure 6(b). Relation between standard enthalpy change and electronegativity of metal in Li(NH$_3$)$_4$Cl, Ca(NH$_3$)$_4$Cl$_2$, Mg(NH$_3$)$_6$Cl$_2$.

Pauling electronegativities of different elements have the following values: K(0.82), Na(0.93), Sr(0.95), Li(0.98), Ca(1.00), Mg(1.31), Mn(1.55), Ni(1.91) and F(3.98), Cl(3.16), Br(2.96), I(2.66) [42]. The lower equilibrium pressure would be obtained from the large electronegativity of metal elements in the metal ammine complex salts (Table 1) [17]. Metal cation dependences of metal halide-NH$_3$ systems (2LiCl-2NH$_3$, 2NaCl-2NH$_3$, 2KCl-2NH$_3$, MgCl$_2$-2NH$_3$, CaCl$_2$-2NH$_3$) were studied by *ab initio* calculations. Figure 6 (a) shows relation between the calculated absorption energy and electronegativity of the metal element [43]. The absorption energy increases with the electronegativity of metal. NH$_3$ absorbs on metal chlorides (MCl) directing its N atom to M, and absorption energy of NH$_3$ depends on M atoms. Anion interaction of M-NH$_3$ (M: Li, Na, K, Mg, Ca) mainly comes from NH$_3$-anion repulsion [43]. It will be considered that absorption energy between metal halide (MX) and NH$_3$ increases in the order (MF<MCl<MBr<MI) (M: Li, Na, K, Mg, Ca etc.). Figure 6 (b) shows relation between the standard enthalpy change and electronegativity. The absolute values increase with electronegativity of Li, Ca and Mg. Those values correspond to the calculated absorption energy. M and lone electron pair of NH$_3$ form coordinate bond. We found that the absolute value of the standard enthalpy change increases as the electronegativity of metal and

nitrogen (3.04) becomes closer.

3.2 Complex hydrides

The reaction of borohydrides with anhydrous NH_3 vapor to form metal ammine complex salts as shown in the following equation [17, 19, 44-50]

$$M(BH_4)_m + nNH_3 \rightarrow M(NH_3)_n(BH_4)_m \quad (5)$$

where, M: Li, Na, Mg, Ca, n=1-6, m=3(Al), m=2(Mg, Ca), m=1(Li, Na)

Figure 7 shows experimental pressure-composition (P-C) isotherms for $NaBH_4$-NH_3 system [48]. NH_3 absorption and desorption reactions of sodium borohydride is reversible at room temperature [48, 49]. There is no hysteresis behavior. The reaction is explained by the equation.

$$NaBH_4 + 2NH_3 \leftrightarrow Na(NH_3)_2BH_4 \quad (6)$$

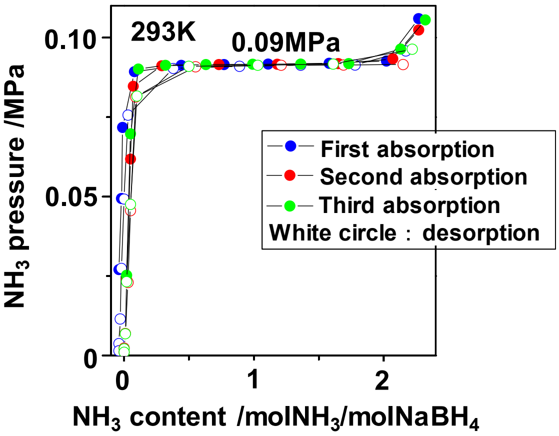

Figure 7. Pressure-composition (P-C) isotherms for $NaBH_4$-NH_3 system [36].

$NaBH_4$ can reversibly store 47 wt% of NH_3 under NH_3 plateau pressure of 90000-96000 Pa at 293 K [17, 19, 48, 49]. KBH_4 shows no NH_3 absorption under 0.8 MPa NH_3 pressure (Table 2). The plateau pressures of $Mg(BH_4)_2$ and $Ca(BH_4)_2$ absorbed NH_3 are 57-2000 and 37-6500 Pa, respectively. These pressures depend on the coordination numbers.

Table 2. Theoretical gravimetric NH_3 density, plateau pressure, standard enthalpy and entropy changes in borohydride-NH_3 systems (metal borohydride ammine complex salts), ammonia borane-NH_3 system and NH_3 gas.

Borohydrides, ammonia borane and ammonia	**Metal ammine complexes and ammonia borane absorbed NH_3 /g/cm^3**	**Theoretical gravimetric NH_3 density /wt%**	**Plateau pressure /Pa(293-298K)**	**Standard enthalpy change ΔH^0 /kJ/molNH$_3$**	**Standard entropy change ΔS^0 /J/KmolNH$_3$**
$NaBH_4$	**$Na(NH_3)_2BH_4$**	**47.4**	**90000 (293K) [17,48] 93000 (293K) [49] 96000 (293K) [19]**	**-29 [17]**	**-98 [17]**
$LiBH_4$	**$Li(NH_3)BH_4$ $Li(NH_3)_2BH_4$ $Li(NH_3)_3BH_4$**	**43.9 61.0 70.1**	**2000 (293K) [19] 6000 (293K) [19] 12000 (293K) [19]**	**-44.8 [44] -45.2 [44] -**	**- -**
KBH_4	**-**	**-**	**>800000 (293K) [17,19]**	**-**	**-**
$Mg(BH_4)_2$	**$Mg(NH_3)(BH_4)_2$ $Mg(NH_3)_2(BH_4)_2$ $Mg(NH_3)_5(BH_4)_2$**	**24.0 38.7 61.2**	**57 (293K) [17,19] 96 (293K) [17,19] 2000 (293K) [17,19]**	**- - -**	**- - -**
$Ca(BH_4)_2$	**$Ca(NH_3)(BH_4)_2$ $Ca(NH_3)_2(BH_4)_2$ $Ca(NH_3)_5(BH_4)_2$**	**19.6 32.8 55.0**	**37 (293K) [17,19] 300 (293K) [17,19] 6500 (293K) [17,19]**	**-52.7 [46] -48.0 [46] -34.9 [46]**	**- -**
$Al(BH_4)_3$	**$Al(NH_3)_6(BH_4)_3$**	**58.8**	**-**	**- [50]**	**-**
NH_3BH_3	**NH_3BH_3-0.7NH_3**	**27.9**	**100000 (296K) [51]**	**-**	**-**
NH_3 gas	**liquid NH_3**	**100**	**850000 (293K) [52] 1000000(298K) [52]**	**-23 [17]**	**-97 [17]**

The gravimetric NH_3 densities of borohydride-NH_3, ammonia borane-NH_3 systems are 20-70 wt%, as shown in Table 2. The plateau pressure also decreases with decreasing of the coordination number. The lower the plateau pressure is, the higher the absolute value of the standard enthalpy change is. Aluminum borohydride reacts with NH_3 to form $Al(BH_4)_3 6NH_3$ and also exhibits ammonia storage capacity of 59 wt% [50].

The NH_3 plateau pressure of metal borohydride ammine complex salts is above 30 Pa which doesn't satisfy the regulation value of the odor control law at industrial area in Japan.

The standard enthalpy change (standard heat of formation) ΔH^0 and the standard entropy change ΔS^0 of $NaBH_4$ were -29 kJ/molNH$_3$ and -98 J/KmolNH$_3$, respectively. The ΔH^0 and the ΔS^0 of NH_3 were -23 kJ/molNH$_3$ and -97 J/KmolNH$_3$, respectively [17]. Those absolute values of the ΔH^0 for $NaBH_4$ are large compared with NH_3. The absolute value of ΔS^0 is similar to the standard entropy change of NH_3 and is smaller than entropy of NH_3 gas (193 J/KmolNH$_3$) [17]. This indicates that the entropy of $NaBH_4$ absorbed NH_3 is similar to the value of liquid NH_3.

Figure 8(a) shows pressure-composition isotherm for $NaBH_4$-NH_3 system with NH_3 content from 0 to above 9 molNH$_3$/molNaBH$_4$. The NH_3 vapor pressure increases above the NH_3 content of 2. This corresponds to the solubility of $NaBH_4$ in NH_3 (solubility of

$NaBH_4$ in NH_3: 104 g/100gNH_3, NH_3 content: 2.1 molNH_3/mol$NaBH_4$) [53]. It has been reported that liquefaction of NH_3 in $NaBH_4$ between the NH_3 content of 0 to 9 molNH_3/mol $NaBH_4$ is clarified by NMR and FT-IR [49].

Figure 8(b) shows Pressure-composition (P-C) isotherms for NH_3BH_3-NH_3 system [51]. Ammonia borane also absorbs 27 wt % of NH_3 under NH_3 pressure of 10^5 Pa at 296 K. The NH_3 vapor pressure increases drastically above NH_3 content of 0.7 molNH_3/molNH_3BH_3. This value corresponds to the solubility of NH_3 in NH_3BH_3 (solubility of NH_3BH_3 in NH_3: 260 g/100gNH_3, NH_3 content: 0.7 molNH_3/molNH_3BH_3) [54]. This indicates that NH_3BH_3 absorbed NH_3 is liquid above NH_3 content of 0.7 molNH_3/molNH_3BH_3.

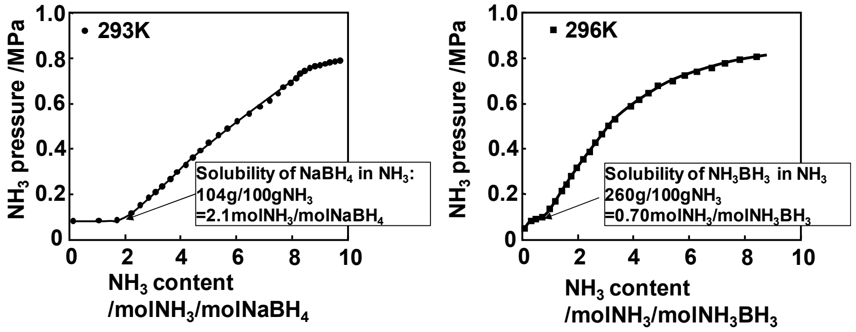

(a) (b)

Figure 8. Pressure-composition (P-C) isotherms for $NaBH_4$-NH_3 and NH_3BH_3-NH_3 systems [17, 19, 48, 49, 51-54]

3.2.1 Standard enthalpy difference and electronegativity of metal in metal borohydride-NH_3 systems

Metal cation dependence of metal borohydride-NH_3 systems (2$LiBH_4$-2NH_3, 2$NaBH_4$-2NH_3, 2KBH_4-2NH_3, $Mg(BH_4)_2$-2NH_3, $Ca(BH_4)_2$-2NH_3) were studied by *ab initio* calculations [43]. Figure 9(a) shows relation between calculated absorption energy and electronegativity of metal elements.

The absorption energy increases with the electronegativity. NH_3 absorbs on metal borohydrides (MBH_4) directing its N atom to M, and absorption energy of NH_3 depends on M atoms. The absolute value also increases with electronegativity, as shown in Figure 9(b). It is indicated that the absolute value of the standard enthalpy change increases as the electronegativity of metal increases, which is similar to the NH_3 absorption in metal halides.

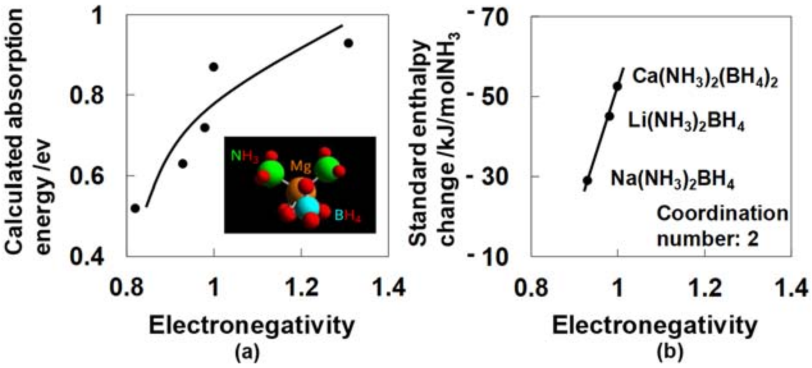

Figure 9(a). Relation between calculated absorption energy and electronegativity of metal in $2LiBH_4$-$2NH_3$, $2NaBH_4$-$2NH_3$, $2KBH_4$-$2NH_3$, $Mg(BH_4)_2$-$2NH_3$, $Ca(BH_4)_2$-$2NH_3$, Figure 9(b). Relation between standard enthalpy change and electronegativity of metal in $Na(NH_3)_2BH_4$, $Li(NH_3)_2BH_4$, $Ca(NH_3)_2BH_4$.

3.3 Proton-based materials

Proton-based materials including H^+, react with lone electron pair of NH_3 in the atmosphere and in NH_3 water to form ammonium ion at room temperature [55-59]. Proton-based materials can yield NH_4^+ by the following equation.

$$MH_n + nNH_3 \rightarrow M(NH_4)_n \tag{7}$$

M: NH_4SO_4, $Zr(PO_4)_2(H_2O)$
n: 1, (NH_4SO_4)
n: 2, [$Zr(PO_4)_2\cdot(H_2O)$]

Table 3 shows NH_3 densities and standard enthalpy and entropy changes in proton-based materials. The solid proton-based materials such as ammonium sulfate (NH_4HSO_4), acid impregnated charcoal, zirconium bis(mono-hydrogen phosphate) monohydrate [α-$Zr(HPO_4)_2\cdot(H_2O)$](α-zirconium phosphate) (α-ZrP) absorbed NH_3 have low NH_3 vapor pressure of 0.2 Pa or below [14, 55-57, 59].

The NH_3 absorption reaction is exothermic. The standard enthalpy changes ΔH^0 of the proton-based materials is -109 kJ/molNH_3 [59]. The absolute values of the ΔH^0 are large compared with the metal halides and metal borohydrides.

Table 3. Theoretical gravimetric NH_3 density, equilibrium NH_3 vapor pressure, standard enthalpy and entropy changes in proton-based material-NH_3 system (ammonium ion-based materials).

Proton-based materials	**Ammonium ion-based materials**	**Theoretical gravimetric NH_3 density /wt%**	**Equilibrium pressure /Pa(293-298K)**	**Standard enthalpy change ΔH^0 /kJ/molNH_3**	**Standard entropy change ΔS^0 /J/KmolNH_3**
Ammonium hydrogen sulfate NH_4HSO_4	**Ammonium sulfate $(NH_4)_2SO_4$**	**12.9**	**3.51×10^{-5} *2 (298K) 4×10^{-8} (4×10^{-9}-4×10^{-7}) (298K) [14]**	**-109 [59]**	**-191 [59]**
Acid impregnated charcoal	-	**(3.2) *1**	**0.01 (298K) [55]**	**-**	**-**
α-Zirconium bis(mono-hydrogen phosphate) monohydrate α-$Zr(HPO_4)_2(H_2O)$	**α-Zirconium bis(ammonium phosphate) monohydrate α-$Zr(NH_4PO_4)_2(H_2O)$**	**10.2(6.64 mmol/g)[56] (10.2) *1[57]**	**≈0 [56] 0.2 [57] (293K)**	**-**	**-**

***1 Experimental value *2 Calculated value from ΔH^0 and ΔS^0**

H^+ in NH_4HSO_4 reacts with lone electron pair of NH_3 to form coordinate bond. The large standard enthalpy change may be due to the fact that the electronegativity difference between H (2.20) and N (3.04) is small compared with that between metal (Mg, Ca etc.) and N. The absolute value of the standard entropy change for the solid NH_4HSO_4 is 191 J/KmolNH_3 and similar to the entropy of NH_3 gas (193 J/KmolNH_3 at 298 K) [17, 59]. The absolute values is large compared with metal halides and metal borohydrides.

3.4 Porous materials

Materials with high surface area and porous structure seem to be very promising for NH_3 storage. Gravimetric NH_3 densities, equilibrium pressure and the standard enthalpy change in porous materials are shown in Table 4. The adsorption isotherm for the activated carbon shows Langmuir type equation. By the Clausius-Clapeyron equation, the standard enthalpy changes on the activated carbon are estimated to be -8 to -17 kJ/molNH_3 [60]. The absolute values are smaller than those of metal halides, complex hydride and proton-based materials. It has been reported that adsorption of NH_3 gas on activated carbon is mainly based on physisorption such as van der Waals force [60].

The standard enthalpy changes on the zeolite 13X are -30 to -49 kJ/molNH_3 [62]. The values are similar to those of $Li(NH_3)_4Cl$, $Ca(NH_3)_8Cl_2$, $Mn(NH_3)_8Cl_2$, $Sr(NH_3)_8Cl_2$,

$Ba(NH_3)_8Cl_2$, $Li(NH_3)_2BH_4$, $Na(NH_3)_2BH_4$ and $Ca(NH_3)_2(BH_4)_2$. NH_3 can be adsorbed on zeolite by electrostatic attraction [63].

Covalent organic frameworks (COFs) are porous crystalline materials composed of light elements linked by strong covalent bonds. It has been reported that a member of the covalent organic framework family, COF-10, shows the highest uptake capacity (15 mmol/ g, 298 K, 0.1 MPa) of any porous material, including microporous 13X zeolite (9 mmol/g), Amberlyst 15 (11 mmol/g) and mesoporous silica, MCM-41 (7.9 mmol/g) [64].

Prussian blue is a historical pigment synthesized for the first time at the beginning of 18th century. Here we demonstrate that the historical pigment exhibits surprising adsorption properties of gaseous NH_3. Prussian blue shows 12.5 mmol/g of NH_3 capacity at 0.1 MPa [65]. The respective capacities of cobalt hexacyanocobaltate (CoHCC) and copper hexacyanoferrate (CuHCF) were raised to 21.9 and 20.2 mmol/g, respectively [65].

Table 4. Gravimetric NH_3 density, equilibrium NH_3 vapor pressure and standard enthalpy change in porous materials and water.

Porous materials and water	**Experimental gravimetric NH_3 density /wt%**	**Equilibrium pressure /Pa(293-323K)**	**Standard enthalpy change ΔH^0 /kJ/molNH_3**
Activated carbons	**0.39 (0.15-0.62) 0.1**	**50 (303K) [60] 10 (298K) [61]**	**-8 to -17 [60] -**
Zeolite(Li-X) Zeolite 13X 3A Y-Zeolite	**5.0 5.6 (78.8 ml/g) 3.2 (43.8 ml/g) 10.6 (4.59-9.34 mmol/g)**	**8 (293K) [6] 50 (303K) [62] 50 (303K) [62] 40000 (323K) [63]**	**- -30 to -49 [62] - -**
Sepiolite	**2.4**	**8.4 (298K) [61]**	**-**
COF-10 Zeolite 13X Amberlyst 15 MCM-41	**20.3 (15 mmol/g) 13.3 (9 mmol/g) 15.8 (11 mmol/g) 11.9 (7.9 mmol/g)**	**100000 (298K) [64] 100000 (298K) [64] 100000 (298K) [64] 100000 (298K) [64]**	**- - -**
Prussian blue cobalt hexacyanocobaltate (CoHCC) Copper hexacyanoferrate (CuHCF)	**17.6 (12.5 mmol/g) 27.2 (21.9 mmol/g) 25.6 (20.2 mmol/g)**	**100000 (298K) [65] 100000 (298K) [65] 100000 (298K) [65]**	**- - -**
Water	**32**	**100000 (298K) [66]**	**-30 [67]**

The gravimetric NH_3 densities of those porous materials are 0.1-27 wt%, as shown in Table 4. The equilibrium pressure is 8-10^5 Pa, which is high compared with the vapor pressure of 0.2 Pa based on the regulation value of the offensive odor control law at industrial area in Japan.

3.5 Water

The gravimetric NH_3 density in NH_3 water is 32 wt% at 0.1 MPa and 298 K as shown in Table 4 [66]. The standard enthalpy change is -30 kJ/molNH_3 [67]. In the NH_3 water, positive charged $H^{\delta+}$ of H_2O and $N^{\delta-}$ of NH_3 form hydrogen bond [13]. It is well known that large amount of water is a NH_3 absorbent in the plant facilities [68] to suppress the leaked NH_3 because of the large solubility [66, 67] and the large diffusion coefficient in water (1.5×10^{-5} cm^2/sec at 293 K) [59]. The large diffusion coefficient will be based on the low viscosity of water 1 mPa·s at 293 K compared with the solid like glass (10^{14} Pa·s at 773 K) [69, 70]. Figure 10 (a) shows solubility of NH_3 in water as a function of temperature [66]. The solubility of NH_3 is high and 46 g/100gH_2O (32 wt%) at the NH_3 vapor pressure of 0.1 MPa and 298 K (Table 4). The vapor pressure decreases with temperature [66]. Vapor concentration (ppm) is obtained by 10 times of vapor pressure (Pa). NH_3 vapor concentration and NH_3 concentration in the water solution have similar high values at 298 K as shown in Figure 10 (b) [68]. This indicates that NH_3 vapor concentration corresponds to NH_3 concentration in NH_3 water.

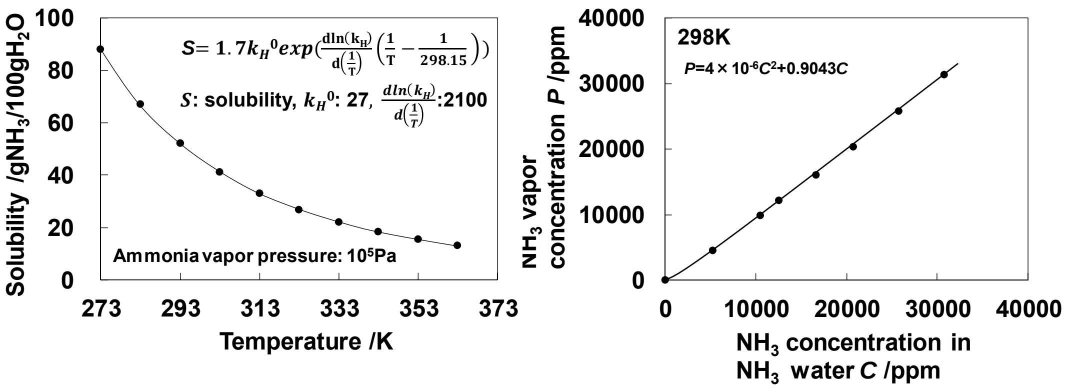

(a) (b)

Figure 10. Solubility of NH_3 in water (NH_3 vapor pressure: 10^5 Pa, NH_3 vapor concentration: 10^6 ppm) and NH_3 vapor concentration as a function of NH_3 concentration in NH_3 water [66, 67].

4. NH_3 vapor pressure and NH_3 storage densities.

Figure 11 shows experimental and calculated NH_3 vapor pressures of metal ammine complex salts, ammonium ion-based materials, porous materials adsorbed NH_3, NH_3 water and NH_3. The NH_3 vapor pressure is in the range of 10^{-8} Pa to 10^5 Pa and is classified into three categories: (1) NH_3 vapor pressure ≤ 0.2Pa, (2) 0.2Pa < NH_3 vapor pressure ≤ 1000 Pa, (3) 1000 Pa <NH_3 vapor pressure <200000 Pa. $Zr(NH_4PO_4)_2\cdot(H_2O)$, $(NH_4)_2SO_4$, NH_3 adsorbed impregnated charcoal, $Mg(NH_3)Cl_2$, $Mg(NH_3)_2Cl_2$, $Mn(NH_3)Cl_2$ and $Mn(NH_3)Br_2$ have low NH_3 vapor pressure of 0.2 Pa or below.

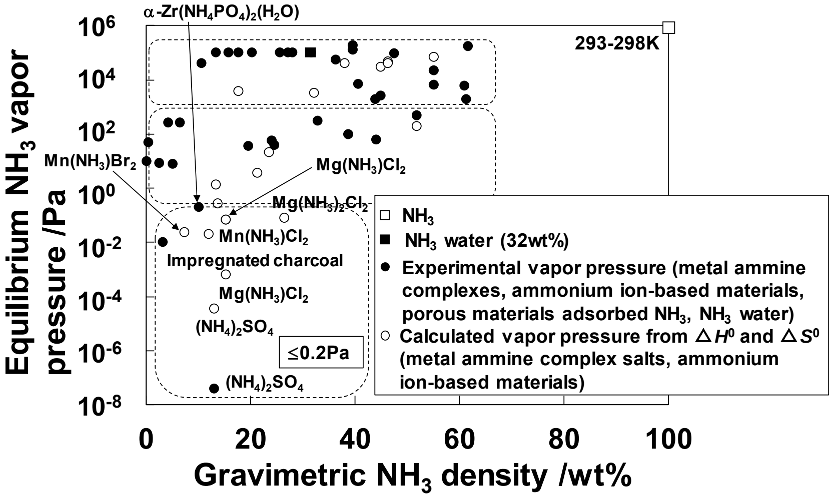

Figure 11. Equilibrium NH_3 vapor pressure and gravimetric NH_3 densities of metal ammine complex salts, ammonium ion-based materials, porous materials adsorbed NH_3 and NH_3 water.

The densities of $(NH_4)_2SO_4$, $Mg(NH_3)_6Cl_2$, $Mg(NH_3)_2Cl_2$, $Ca(NH_3)_8Cl_2$, $Mn(NH_3)_6Cl_2$, $Sr(NH_3)_8Cl_2$, $Ni(NH_3)_2Cl_2$, $Ni(NH_3)_2Br_2$, $Mn(NH_3)_2Cl_2$, $Mn(NH_3)_2Br_2$, $Mn(NH_3)_6Br_2$, α-$Zr(NH_4PO_4)_2{\cdot}(H_2O)$ and NH_3 water (32 wt%) are 1.77 [59], 1.25 [24], 1.70 [19], 1.19 [24], 1.41 [24], 1.30 [25], 2.31 [21], 3.17 [21], 2.06 [26], 2.84 [26], 1.80 [26], 2.39 [71] and 0.89 [59, 72] g/cm^3, respectively. These materials are classified as a solid or as a liquid. The volumetric NH_3 densities of solid materials are assumed that those packing ratio is 50 % [1].

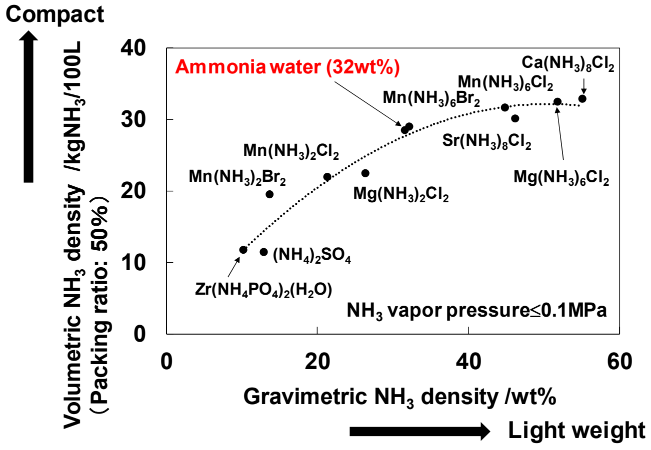

Figure 12. Gravimetric and volumetric NH_3 densities of NH_3 storage materials such as metal ammine complex salts, $(NH_4)_2SO_4$, α-$Zr(NH_4PO_4)_2{\cdot}(H_2O)$ and NH_3 water.

Figure 12 shows volumetric and gravimetric NH_3 densities of metal ammine complex salts, $(NH_4)_2SO_4$, α-$Zr(NH_4PO_4)_2\cdot(H_2O)$ and NH_3 water. Volumetric NH_3 densities increase with gravimetric NH_3 densities, approaching constant value of 33 kgNH$_3$/100L. The volumetric NH_3 densities of NH_3 water at the gravimetric NH_3 density of 32 wt% is calculated to be 28 kg NH$_3$/100L. NH_3 water has high gravimetric and volumetric NH_3 densities, although the NH_3 vapor pressure is 0.1 MPa.

The theoretically calculated densities of metal ammine complex salts, $(NH_4)_2SO_4$, α-$Zr(NH_4PO_4)_2\cdot(H_2O)$ and NH_3 water d_c can be calculated by the following addition relationship [1].

$$d_c = \sum_{i=1}^{n} \frac{x_i M_i}{V} \tag{8}$$

$$V = \sum_{i=1}^{n} \frac{x_i M_i}{d_i} \tag{9}$$

Here, suffix *i* indicates certain kinds of atoms. *x, M, d* and *V* are molecular ratio, molecular weight, density and volume composed of the NH_3 storage materials before absorption, respectively. The densities of NH_4HSO_4, $MgCl_2$, $CaCl_2$, $MnCl_2$, $SrCl_2$, $NiCl_2$, $NiBr_2$, $MnBr_2$, α-$Zr(HPO_4)_2\cdot(H_2O)$, H_2O and $NaBH_4$ are 1.78, 2.33, 2.15, 2.98 3.05, 3.51, 5.10, 4.39, 2.77, 0.997 and 1.07 g/cm^{3}respectively [59, 73]. The molecular weights of NH_4HSO_4, $MgCl_2$, $CaCl_2$, $MnCl_2$, $SrCl_2$, $NiCl_2$, $NiBr_2$, $MnBr_2$, α-$Zr(HPO_4)_2\cdot(H_2O)$, H_2O and $NaBH_4$ are 115, 95.2, 111, 126, 159, 130, 219, 215, 301, 18.0 and 37.8, respectively. The density and molecular weight of liquid NH_3 at 298 K and 1 MPa are 0.603 g/cm^3 and 17.0, respectively. The densities of $(NH_4)_2SO_4$, $Mg(NH_3)_6Cl_2$, $Mg(NH_3)_2Cl_2$, $Ca(NH_3)_8Cl_2$, $Mn(NH_3)_6Cl_2$, $Sr(NH_3)_8Cl_2$, $Ni(NH_3)_2Cl_2$, $Ni(NH_3)_2Br_2$, $Mn(NH_3)_2Cl_2$, $Mn(NH_3)_2Br_2$, $Mn(NH_3)_6Cl_2$, $Mn(NH_3)_6Br_2$, α-$Zr(NH_4PO_4)_2\cdot(H_2O)$, NH_3 water and $NaBH_4$-2.7NH_3 system are calculated by equations (8) and (9).

Figure 13 shows relation between experimental density of solid metal ammine complex salts, ammonium ion-based materials ($(NH_4)_2SO_4$, α-$Zr(NH_4PO_4)_2\cdot(H_2O)$) and the calculated density by addition relationship. In the same figure, experimental and calculated liquid densities of NH_3 water (5 wt%, 0.98 g/cm^3, 10 wt%, 0.96 g/cm^3, 25 wt%, 0.91 g/cm^3, NH_3: 32 wt%, 0.89 g/cm^3)[72] and $NaBH_4$-2.7NH_3 system [48] are also shown.

The experimental solid densities of metal ammine complex salts and ammonium ion-based materials are about 1.3 times of the calculated density, although the experimental density of NH_3 water and $NaBH_4$-2.7NH_3 are similar to the calculated density. This suggests that NH_3 densities in those solid materials are high compared with the liquid NH_3 (0.603 g/cm^3 at 298 K). It is presumed that the NH_3 density in the material having low NH_3 vapor pressure has high value.

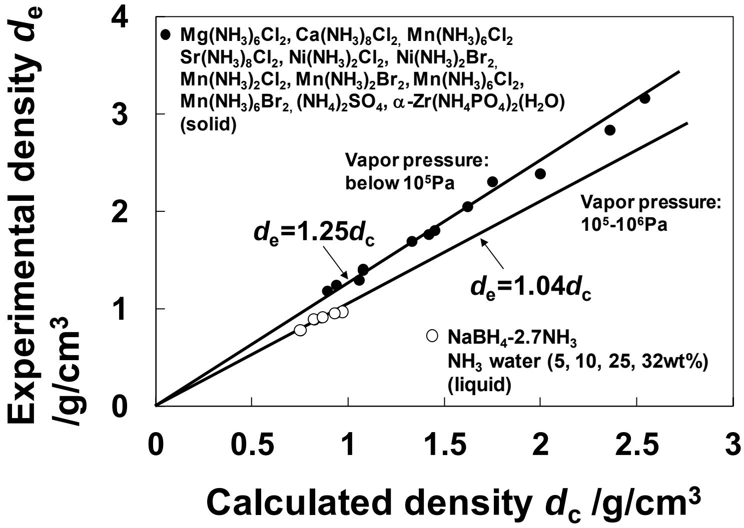

Figure 13. Experimental solid and liquid densities of metal ammine complex salts, α-$Zr(NH_4PO_4)_2(H_2O)$, $NaBH_4$ absorbed NH_3 and NH_3 water as a function of the calculated densities by addition relationship.

5. NH_3 removal system combined water and insoluble proton-based materials

Water has high NH_3 storage densities of 32 wt% and 28 kg/100L among NH_3 storage materials (Figure 12), although water has high equilibrium NH_3 vapor concentration (Figure 11). Insoluble NH_3 storage materials for the vapor concentration (vapor pressure) lowering in the atmosphere will be required to reduce the negative effects on the environment.

$CuSO_4$ forms metal ammine complex salt with low NH_3 vapor pressure below 0.2 Pa, which is soluble in water [40]. Metal halides such as $MgCl_2$ $MnCl_2$ and $MnBr_2$ are soluble in water (Solubility at 298 K, $MgCl_2$: 56.0 g/100gH_2O, $MnCl_2$: 77.3 g/100gH_2O, $MnBr_2$:

151 g/100gH_2O) [59] and it prevents the formation of metal ammine complex salts with low NH_3 vapor pressure below 0.2 Pa. Complex hydrides react with water to generate hydrogen [74-76], as well as the NH_3 plateau pressure above 30 Pa.

Proton-based materials including proton H^+, react with NH_3 vapor of 0.2 Pa or below to form ammonium ion [55-59]. These materials are classified into soluble and insoluble materials in water. NH_4HSO_4 reacts with NH_3 to form $(NH_4)_2SO_4$ and is soluble in water (solubility at 298 K, $(NH_4)_2SO_4$: 76.4 g/100gH_2O). The soluble proton-based materials only converts NH_3 into NH_4^+ and cannot reduce nitrogen concentration in the water solution.

Insoluble proton-based materials absorb NH_3 and the equilibrium pressure is 0.2 Pa or below, as shown in Table 3 and Figure 11. It has been also reported that insoluble α-zirconium phosphate absorbs NH_3 in water and has low nitrogen concentration (NH_3-N) below 1ppm in NH_3 water [77]. Thus, insoluble proton-based materials will be used to remove nitrogen from NH_3 water. α-zirconium phosphate [56, 57, 77], acid-impregnated charcoal [55, 78], proton exchanged zeolite [79] and proton-exchanged montmorillonite [80, 81] will be candidates as insoluble proton-based materials

Figure 14 shows conceptive picture of NH_3 removal system. This system is composed of water and insoluble proton-based materials. Water easily collects leaked NH_3 because the solubility and the diffusion coefficient in water are large. NH_3 molecule can easily diffuse to insoluble proton-based materials, and react with insoluble proton-based

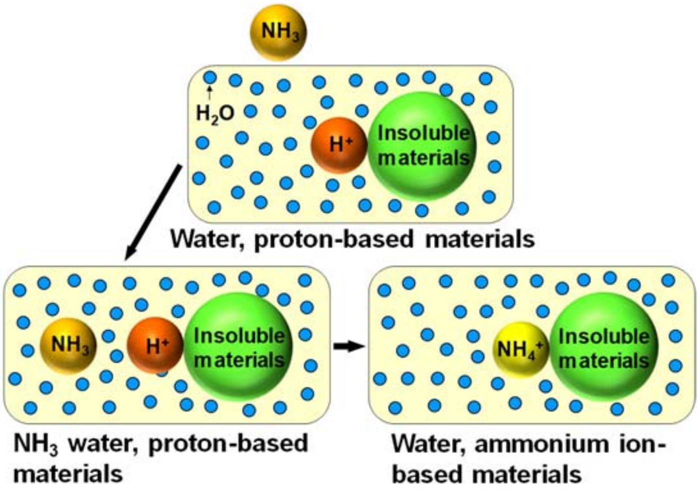

Figure 14. Conceptive picture of NH_3 removal system combined water and insoluble proton-based materials.

materials to form insoluble ammonium ion-based materials. Then nitrogen is removed from water. Therefore the system combined water and insoluble proton-based materials will be candidate to decrease the leaked NH_3 concentration by suppression of water pollution.

6. Conclusion

The gravimetric NH_3 densities such as metal halides, complex hydrides, proton-based materials, porous materials and water were 0.1-70 wt%. The vapor pressure was in the range of 10^{-8} to 10^{5} Pa. The absolute value of the standard enthalpy change increased as the electronegativity of metal and nitrogen becomes closer. The absolute value of the standard entropy change was below 200 J/KmolNH$_3$. Among these materials, water easily collects leaked ammonia because of the large solubility and diffusion coefficient in water. Insoluble proton-based materials were recognized as an attractive NH_3 storage materials because they have a low NH_3 vapor pressure of 0.2 Pa or below, which satisfy the regulation value of the offensive odor control law at industrial area in Japan. It is expected that the NH_3 removal system combined water and insoluble proton-based materials will be candidate to improve the health hazard of NH_3.

Acknowledgments

This work was partially supported by Council for Science, Technology and Innovation (CSTI), Cross-ministerial Strategic Innovation Promotion Program (SIP), “energy carrier” (funding agency: JST). The author is greatly indebted to Professor T. Ichikawa and Associate Professor H Miyaoka of Hiroshima University and Assistant Professor T. Nakagawa of University of the Ryukyus for their help and discussion. And, this work was carried out as a research in Research Center for Nitrogen Recycling Energy Carrier of Hiroshima University.

References

[1] Kojima Y. Hydrogen storage materials for hydrogen and energy carriers. International Journal of Hydrogen Energy. 2019; 44: 18179-18192.

[2] Birol F. The Future of Hydrogen, Seizing today’s opportunities, Report prepared by the IEA for the G20, 82-83, Japan, June 2019.

[3] An GL, Wang LW, Gao J, Wang RZ, A review on the solid sorption mechanism and kinetic models of metal halide-ammonia working pairs. Renewable and Sustainable Energy Reviews. 2018; 91: 783-792.

[4] Cao Z, Osorio NG, Cai X, Feng P, Akhtar F, Carbon-reinforced $MgCl_2$ composites with high

structural stability as robust ammonia carriers for selective catalytic reduction system, Journal of Environmental Chemical Engineering. 2020; 8: 103584.

[5] Miyaoka H, Miyaoka H, Ichikawa T, Ichikawa T, Kojima Y. Highly purified hydrogen production from ammonia for PEM fuel cell. International Journal of Hydrogen Energy. 2018;43:14486-92.

[6] Workplace safety site, Ministry of Health, Labour and Welfare, Japan
ammonia http://anzeninfo.mhlw.go.jp/anzen/gmsds/7664-41-7.html
methylcyclohexane http://anzeninfo.mhlw.go.jp/anzen/gmsds/0977.html
toluene http://anzeninfo.mhlw.go.jp/anzen/gmsds/108-88-3.html

[7] HYDROGEN FUNDAMENTALS
http://www.hysafe.org/download/997/brhs_ch1_fundamentals-version%201_0_1.pdf

[8] The Fertilizer Institute, Nourish, Replenish Grow, HEALTH EFFECTS of AMMONIA http://www.tfi.org/sites/default/files/documents/HealthAmmoniaFINAL.pdf

[9] Occupational Safety and Health Administration, Ammonia Refrigeration,
https://www.osha.gov/SLTC/ammoniarefrigeration/

[10] CAMEO Chemicals, HYDROGEN, REFRIGERATED LIQUID (CRYOGENIC LIQUID), CAS Number 1333-74-0, https://cameochemicals.noaa.gov/chemical/3606

[11] Kojima Y, Ikeda H. 4-5-3 Safety of ammonia as hydrogen and energy carriers. Abstract of Papers, 28th Annual Meeting of the Japan Institute of Energy tournament, August 7, 2019 (Wednesday) to 8 (Thursday) Osaka (Kansai University Senriyama Campus)

[12] Odor Control Law in Japan,
http://www.pref.toyama.jp/sections/1103/reiki_int/reiki_honbun/i001RG00000429.html

[13] Shriver and Atkins. Inorganic Chemistry, 5th revised Edition, (Oxford University Press, 2010), Basolo F, Johnson R C. Coordination Chemistry, Second Edition, Science Reviews Limited, 1986.

[14] Scott W D, Cattell F C R. Vapor pressure of ammonium sulfates. Atmospheric Environment 1979; 13: 307-317.

[15] Asada T, Ohkubo T, Kawata K, Oikawa K. Ammonia adsorption on bamboo charcoal with acid treatment. Journal of Health Science. 2006; 52: 585-589.

[16] Liu C Y, Aika K-i. Ammonia absorption on alkaline earth halides as ammonia separation and storage procedure. Bulletin of the Chemical Society of Japan. 2004; 77: 123-131.

[17] Aoki T, Ichikawa T, Miyaoka H, Kojima Y. Thermodynamics on ammonia absorption of metal halides and borohydrides. Journal of Physical Chemistry C. 2014;118:18412-6.

[18] Aoki T, Miyaoka H, Inokawa H, Ichikawa T, Kojima Y. Activation on ammonia absorbing reaction for magnesium chloride. Journal of Physical Chemistry C. 2015;119:26296-302.

[19] Zhang T, Miyaoka H, Miyaoka H, Ichikawa T, Kojima Y. Review on ammonia absorption

materials: metal hydrides, halides, and borohydrides. ACS Applied Energy Materials. 2018;1:232-42.

[20] Neveu P, Castaing J. Solid-gas chemical heat pumps: Field of application and performance of the internal heat of reaction recovery process, Heat Recovery Systems and CHP. 1993; 13: 233-251.

[21] Leineweber A, Jacobs H. Preparation and crystal structures of $Ni(NH_3)_2Cl_2$ and of two modifications of $Ni(NH_3)_2Br_2$ and $Ni(NH_3)_2I_2$. Journal of Solid State Chemistry. 2000; 152: 381-387.

[22] Elmøe T D, Sørensen R Z, Quaade U, Christensen C H, Nørskov J K, Johannessen T. A high-density ammonia storage/delivery system based on $Mg(NH_3)_6Cl_2$ for SCR–$DeNO_x$ in vehicles. Chemical Engineering Science. 2006; 61: 2618-25.

[23] Klerke A, Christensen CH, Nørskov JK, Vegge T. Ammonia for hydrogen storage: challenges and opportunities. Journal of Materials Chemistry. 2008;18:2304-10.

[24] Sørensen RZ, Hummelshøj JS, Klerke A, Reves JB, Vegge T, Nørskov JK, et al. Indirect, reversible high-density hydrogen storage in compact metal ammine salts. Journal of the American Chemical Society. 2008;130:8660-8.

[25] Fulks G, Fisher G B, Rahmoeller K, Wu M-C, D'Herde E, Tan J. A review of solid materials as alternative ammonia sources for lean NO_x reduction with SCR. SAE International. 2009-01-0907.

[26] Reardon H, Hanlon J M, Grant M, Fullbrook I, Gregory D H. Ammonia uptake and release in the $MnX_2 – NH_3$ (X=Cl, Br) systems and structure of the $Mn(NH_3)_nX_2$ (n = 6, 2) ammines. Crystals. 2012; 2: 193-212.

[27] Lysgaard S, Ammitzbøll AL, Johnsen RE, Norby P, Quaade UJ, Vegge T. Resolving the stability and structure of strontium chloride ammines from equilibrium pressures, XRD and DFT. International Journal of Hydrogen Energy. 2012;37:18927-36.

[28] Jones M O, Royse D M, Edwards P P, David W I F. The structure and desorption properties of the ammines of the group II halides. Chemical Physics. 2013; 427: 38-43.

[29] Kubota M, Matsuo K, Yamanouchi R, Matsuda H. Absorption and desorption characteristics of NH_3 with metal chlorides for ammonia storage, J. Chem. Eng. Jpn. 2014; 47: 542-8.

[30] van Hassel BA, Karra JR, Santana J, Saita S, Murray A, Goberman D, et al. Ammonia sorbent development for on-board H2 purification. Separation and Purification Technology. 2015;142:215-26.

[31] Trudela J, Hosattea S, Ternan M. Solid–gas equilibrium in chemical heat pumps: the NH_3–$CoCl_2$ system. Applied Thermal Engineering. 1999; 19: 495-511.

[32] Bojar H-P, Walter F, Baumgartner J, Färber G. Ammineite, $CuCl_2(NH_3)_2$, a new species containing an ammine complex: mineral data and crystal structure, The Canadian

Mineralogist. 2010; 48: 1359-71.

[33] Wu S, Li TX, Wang RZ, Experimental identification and thermodynamic analysis of ammonia sorption equilibrium characteristics on halide salts. Energy. 2018; 161: 955-962.

[34] Sharma R, Kumar E A, Perfformance evaluation of simple and heat recovery adsorption cooling system using measured NH3 sorption characteristics of halide salts. Applied Thermal Engineering. 2017; 119: 459-471.

[35] Sørby M H, Løvvik O M, Tsubota M, Ichikawa T, Kojima Y, Hauback B C. Crystal structure and dynamics of Mg(ND3)6Cl2. Phys. Chem. Chem. Phys. 2011; 13: 7644–48.

[36] Tekin A, Hummelshøj J S, Jacobsen H S, Sveinbjörnsson D, Blanchard D, Nørskova J K, Vegge T. Ammonia dynamics in magnesium ammine from DFT and neutron scattering. Energy & Environmental Science. 2010; 3: 448-56.

[37] Liu C Y, Aika K-i. Effect of the Cl/Br molar ratio of a $CaCl_2-CaBr_2$ mixture used as an ammonia storage material. Industrial & Engineering Chemistry Research. 2004; 43: 6994-7000.

[38] Liu CY, Aika K-i. Ammonia absorption into alkaline earth metal halide mixtures as an ammonia storage material. Industrial & Engineering Chemistry Research. 2004;43:7484-91.

[39] Nakagawa T, Shiroma M. The crystal structure refinement of Cu(NH3)nSO4 (n=1-5) by synchrotron XRD. Kyushu Synchrotron Light Research Center Prefectural Beamline Usage Report, Assignment number: 1610091PT, BL number:15.

[40] Yasuoka T, Ichinose M, Saito A, Takano J, Mitsuzawa S. A new technique for measuring average concentration of ammonia in the atmosphere for a long time. Journal of the Chemical Society of Japan, Chemistry and Industrial Chemistry. 1985; No.5: 956-960.

[41] Pal P, Nakajima K, Jain A, Miyaoka H, Ichikawa T. Ammonium halides as new ammonia absorption materials (a90452), abstract of papers, World Hydrogen Technologies Convention (WHTC 2019), Tokyo International Forum, June 2-June 7, Tokyo (2019).

[42] Pauling L. The Nature of the Chemical Bond, Third Edition, Cornell University Press (1960), Emsley J, The Elements, Third Edition, Oxford, Clarendon Press, 1998.

[43] Yamane A, Shimojo F, Ichikawa T, Kojima Y. Cation/anion dependence of metal ammine borohydrides/chlorides studied by ab initio calculations, Computational and Theoretical Chemistry. 2014; 1039 C: 71-74.

[44] Sullivan E A, Johnson S. The lithium borohydride-ammonia system: pressure-composition-temperature relationships and densities. The Journal of Physical Chemistry. 1959; 63: 233-8.

[45] Soloveichik G, Her J-H, Stephens PW, Gao Y, Rijssenbeek J, Andrus M, et al. Ammine magnesium borohydride complex as a new material for hydrogen storage: structure and properties of $Mg(BH_4)_2 \cdot 2NH_3$. Inorganic Chemistry. 2008;47:4290-8.

[46] Chu H, Wu G, Xiong Z, Guo J, He T, Chen P. Structure and hydrogen storage properties of

calcium borohydride diammoniate. Chemistry of Materials. 2010;22:6021-8.

[47] Guo Y, Xia G, Zhu Y, Gao L, Yu X. Hydrogen release from amminelithium borohydride, LiBH4·NH3. Chemical Communications. 2010;46:2599-601.

[48] Kojima Y, Aoki T, Miyaoka H, Miyaoka H, Ichikawa T. Ammonia storage using $NaBH_4$. Abstract of Papers. 35th Annual Meeting of Hydrogen Energy Systems Society of Japan, December 3 (Thursday) to 4 (Friday) 2015, Tokyo (Tower Hall Funabori).

[49] Nakajima K, Miyaoka H, Kojima K, Ichikawa T, Kojima Y. Operando spectroscopic analyses for the ammonia absorption process of sodium borohydride, Chemical Communications; 2019; 55, 2150-2153.

[50] Guo Y, Yu X, Sun W, Sun D, Yang W. The hydrogen-enriched Al–B–N system as an advanced solid hydrogen-storage candidate. Angewandte Chemie International Edition. 2011; 50: 1087-1091.

[51] Kawauchi H, To K, Kojima Y, Ichikawa T. Ammonia storage and release material, ammonia storage and release device, and exhaust gas purification system. JP 2014-43359.

[52] NIST Chemistry WebBook, SRD 69, Thermophysical Properties of Ammonia https://webbook.nist.gov/cgi/fluid.cgi?ID=C7664417&Action=Page

[53] Walbridge J. Metal tetrahydroborates, Progress in Inorganic Chemistry; 1970: 11, 99-231.

[54] Stephens F H, Pons V, Baker R T, Ammonia –borane: the hydrogen source par excellence ?, Dalton Transactions; 2007, 2613-2626.

[55] Nishino H. Removal of offensive odor by impregnated activated carbon. Environmental Technology Japan. 1990: 19: 643-645.

[56] Tsuhako M, Nakayama H. Properties of layered phosphate as functional material. Journal of the Society of Inorganic Materials, Japan. 2000; 7: 679-84.

[57] Kojima Y. Final Report, Emergency ammonia adsorption method, Cross-ministerial Strategic Innovation Promotion Program (SIP), “energy carrier”, Japan. 2019, April 2018-March 31, https://www.jst.go.jp/sip/k04.html, Kojima Y, Yamaguchi M, Ichikawa T, Miyaoka H. Proton-based ammonia storage materials for nitrogen recycling hydrogen and energy carriers. Abstract of Papers. 2019 Frontiers in Materials Processing, Application, Research & Technology (2019 FiMPART), Ahmedabad, India, December 15 (Monday) to 18 (Wednesday), 2019.

[58] Turco M, Ciambelli P, Bagnasco G, La Ginestra A, Galli P, Ferragina C. TPD study of NH3 adsorbed by different phases of zirconium phosphate. Journal of Catalysis. 1989; 117: 355-61.

[59] Haynes W M. Editor-in-Chief: CRC Handbook of Chemistry and Physics, 97th Edition, (CRC Press 2016-2017).

[60] Miyoshi T, Boki K, Tanada S. Studies on the adsorption removal of ammonia gas 1)

adsorption of ammonia gas on several kinds of activated carbons. Japan Journal of Industrial Health. 1976; 18: 169-176.

[61] Sugiura M, Fukumoto K, Inagaki S. Adsorption of odorous vapors by sepiolite. Toyota Central R&D Review. Japan 1993; 28: 43-52.

[62] Miyoshi T, Boki K, Tanada S. Studies on the adsorption removal of ammonia gas 2) adsorption of ammonia gas on several kinds of zeolites. Japan Journal of Industrial Health. 1977; 19: 87-91.

[63] Liu C Y, Aika K-i. Ammonia adsorption on ion exchanged Y-zeolites as ammonia storage material. Journal of the Japan Petroleum Institute, 2003; 46: 301-7.

[64] Doonan C J. Tranchemontagne D J, Glover T G, Hunt J R, Yaghi O M. Exceptional ammonia uptake by a covalent organic framework. Nature Chemistry. 2010; 2: 235-7.

[65] Takahashi A, Tanaka H, Parajuli D, Nakamura T, Minami K, Sugiyama Y, Hakuta Y, Ohkoshi S, Kawamoto T. Historical pigment exhibiting ammonia gas capture beyond standard adsorbents with adsorption sites of two kinds. Journal of the American Chemical Society. 2016; 138: 6376-79.

[66] NIST Chemistry WebBook, SRD 69.
https://webbook.nist.gov/cgi/cbook.cgi?ID=C7664417&Mask=10

[67] Chemical Engineering Handbook, Rev. 6 Edition. The Society of Chemical Engineers, Japan, Maruzen (Co., Ltd.) p. 81 1999,
http://ebw.eng-book.com/pdfs/879040e33a05a0e5f1cb85580ef77ad1.pdf

[68] Ministry of Economy, Trade and Industry, About the operation of the functional standards of the General High Pressure Gas Safety Regulations, Ministry of Economy, Trade and Industry, Agency for Natural Resources and Energy, Nuclear Safety and Security Bureau, NISA 69-70, https://www.meti.go.jp/policy/tsutatsutou/tuuti1/TS1-1.pdf

[69] Einstein A, Investigation on the theory of the brownian movement. Annalen der Physik, 1905; 17: 549-560, http://www.slab.phys.nagoya-u.ac.jp/uwaha/einstein1.pdf

[70] Napolitano A, Hawkins EG. Viscosity of a standard soda-lime-silica glass, Journal of Research of the National Bureau of Standards-A Physics and Chemistry. 1964; 68A; 439-48.

[71] Clearfield A, Troup J M. On the mechanism of ion exchange in crystalline zirconium phosphates. VII. The crystal structure of α-zirconium bis(ammonium orthophosphate) monohydrate1; The journal of physical chemistry, 1973; 77: 243-247.

[72] Specific Gravity of Aqua Ammonia, Inyo Process
https://inyoprocess.com/images/chem_appl/aqua_ammonia_specific_gravity_chart.pdf

[73] Ludmila S, Vladimir P. A contribution to the structure of crystalline Zr(HPO4)2 · H2O, Journal of the Less-Common Metals, 1966; 10:130-132.

[74] Amendola SC, Sharp-Goldman SL, Janjua MS, Spencer NC, Kelly MT, Petillo PJ, et al. A

safe, portable, hydrogen gas generator using aqueous borohydride solution and Ru catalyst. International Journal of Hydrogen Energy. 2000;25:969-75.

[75] Kojima Y, Suzuki K, Fukumoto K, Sasaki M, Yamamoto T, Kawai Y, et al. Hydrogen generation using sodium borohydride solution and metal catalyst coated on metal oxide. International Journal of Hydrogen Energy. 2002;27:1029-34.

[76] Xu Q, Chandra M. A portable hydrogen generation system: Catalytic hydrolysis of ammonia–borane. Journal of Alloys and Compounds. 2007;446-447:729-32.

[77] Yamaguchi M, Ichikawa T, Miyaoka H, Nakajima K, Zhang T, Miyaoka H, Kojima Y. 4-5-4 Ammonia absorption properties of proton-based solid acid. Abstract of Papers, 28th Annual Meeting of the Japan Institute of Energy tournament, August 7, 2019 (Wednesday) to 8 (Thursday) Osaka (Kansai University Senriyama Campus)

[78] Kim K H, Shin O S. Adsorption of ammonia on the sulfuric acid treated ACF. Carbon Science. 2001; 2: 109-112.

[79] Dietrch M, Rauch D, Simon U, Porch A, Moos R. Ammonia storage studies on H-ZSM-5 zeolites by microwave cavity pertubation: correlation of dielectric properties with ammonia storage. Journal of Sensors and Sensor Systems, 2015; 4: 263-269.

[80] Zeynizadeh B, Rahmani S, Ilkhanizadeh S. Strongly proton exchanged montmorillonite K10 (H+-Mont) as a solid acid catalyst for highly efficient and environmental benign synthesis of biscoumarins via tandem Knoevenagel–Michael reaction. Polyhedron. 2019; 168: 48-56.

[81] Kojima Y. Miyaoka H, Zhang T. Ammonia detoxification liquid and ammonia detoxification method. JP2019-89035.